

# High-throughput Execution of Hierarchical Analysis Pipelines on Hybrid Cluster Platforms

George Teodoro, Tony Pan, Tahsin M. Kurc, Jun Kong, Lee A. D. Cooper, and Joel H. Saltz

Center for Comprehensive Informatics, Emory University, Atlanta, GA 30322

Email: {george.teodoro, tony.pan, tkurc, jun.kong, lee.cooper, jhsaltz}@emory.edu

**Abstract**—We propose, implement, and experimentally evaluate a runtime middleware to support high-throughput execution on *hybrid* cluster machines of large-scale analysis applications. A hybrid cluster machine consists of computation nodes which have multiple CPUs and general purpose graphics processing units (GPUs). Our work targets scientific analysis applications in which datasets are processed in application-specific data chunks, and the processing of a data chunk is expressed as a hierarchical pipeline of operations. The proposed middleware system combines a bag-of-tasks style execution with coarse-grain dataflow execution. Data chunks and associated data processing pipelines are scheduled across cluster nodes using a demand driven approach, while within a node operations in a given pipeline instance are scheduled across CPUs and GPUs. The runtime system implements several optimizations, including performance aware task scheduling, architecture aware process placement, data locality conscious task assignment, and data prefetching and asynchronous data copy, to maximize utilization of the aggregate computing power of CPUs and GPUs and minimize data copy overheads. The application and performance benefits of the runtime middleware are demonstrated using an image analysis application, which is employed in a brain cancer study, on a state-of-the-art hybrid cluster in which each node has two 6-core CPUs and three GPUs. Our results show that implementing and scheduling application data processing as a set of fine-grain operations provide more opportunities for runtime optimizations and attain better performance than a coarser-grain, monolithic implementation. The proposed runtime system can achieve high-throughput processing of large datasets – we were able to process an image dataset consisting of 36,848 4Kx4K-pixel image tiles at about 150 tiles/second rate on 100 nodes.

## I. INTRODUCTION

The processing power and memory capacity of graphics processing units (GPUs) have rapidly and significantly improved in recent years. Contemporary GPUs provide extremely fast memories and massive multi-processing capabilities, exceeding those of multi-core CPUs. The application and performance benefits of GPUs for general purpose processing have been demonstrated for a wide range of applications [1]. As a result, CPU-GPU equipped machines are emerging as viable high performance computing platforms for scientific computation [2]. More and more supercomputing systems are being built with *hybrid* computing nodes that have multi-core CPUs and multiple GPUs. This trend is also fueled by the availability of programming abstractions and frameworks, such as CUDA [3] and OpenCL [4], that have reduced the complexity of porting computational kernels to GPUs. Nevertheless, taking advantage of hybrid platforms for scientific computing

still remains a challenging problem. An application developer needs to deal with the efficient distribution of computational workload not only across cluster nodes but also among multiple CPU cores and GPUs, which have different performance characteristics and memory capacities, on a hybrid node. The developer also has to take into account potential performance variability across application operations. Operations ported to the GPU will not all have the same amount of performance gains. Some operations are more suitable for massive parallelism and generally achieve higher GPU-vs-CPU speedups than other operations. In addition, the application developer has to minimize data copy overheads when data have to be exchanged between application operations. These challenges often lead to underutilization of the power of hybrid platforms.

In this work we investigate the design and implementation of runtime middleware support to address these issues in the context of large-scale scientific data analysis applications.

Analysis of large datasets is a critical, yet challenging component of scientific studies, because of dataset sizes and the computational requirements of analysis applications. Sophisticated sensors enable scientists in biomedicine and earth systems sciences to perform high resolution measurements of objects under study rapidly. Similarly, leadership scale machines at national laboratories and supercomputer centers have made it possible for researchers to carry out large scale simulations of complex physical phenomena and generate terabytes of data per simulation run. Processing a large dataset can take very long time on even high end workstations. Moreover, a dataset may be analyzed multiple times with different analysis parameters and algorithms to explore different scientific questions, to carry out sensitivity studies, and to quantify uncertainty and errors in analysis results.

While the types of operations and algorithms employed by a scientific project for data analysis will be specific to the objectives of the project, scientific data analysis applications exhibit common data access and processing patterns. Large datasets can often be processed in a set of *data chunks*, where each chunk represents an application-specific (or user-defined) portion of the dataset; in a large image dataset, for instance, each image or an image tile can be a data chunk. Common processing patterns include bag-of-tasks execution [5], generalized reduction and MapReduce patterns [6], and coarse-grain dataflow patterns [7], [8], [9], [10], [11], [12], [13]. In a bag-of-task style execution, application-specific (or user-defined)

arXiv:1209.3332v1 [cs.DC] 14 Sep 2012

chunks of a dataset are processed concurrently. MapReduce has gained popularity in recent years as a framework to support large scale data processing that can be expressed as Map and Reduce operations. Some analysis methods, on the other hand, are more appropriately expressed and executed as a pipeline of operations. For instance, segmentation of a nucleus consists of several steps including creation of image masks, shape creation and morphing, and determination of boundaries. This type of processing can be described more naturally using a coarse-grain dataflow (or filter-stream) pattern [7], in which application processing is carried out as a network of components connected through logical pipes. Each component performs a portion of the application-specific processing, and interactions between the components are realized by flow of data and control information.

In prior work, Mars [14] and Merge [15] evaluated the cooperative use of CPUs and GPUs to speedup MapReduce computations. Mars performed an initial evaluation on the benefits of partitioning Map and Reduce tasks between CPU and GPU statically. Merge extended that approach with dynamic distribution of work at runtime. The Qilin [16] system further proposed an automated methodology to map computation tasks to CPUs and GPUs. Unfortunately, neither of these solutions (Mars, Merge, and Qilin) are able to take advantage of distributed systems. Some projects more recently focused on execution in distributed CPU-GPU equipped platforms [17], [18], [19], [20], [21], [22], [23], [24], [25]. Ravi et al. [18], [20] proposed techniques for automatic translation of generalized reductions to CPU-GPU environments via compiling techniques, which are coupled with runtime support to coordinate execution. The runtime system techniques introduced a number of auto-tuning approaches to partition tasks among CPUs and GPUs for generalized reduction operations. The work developed by Hartley et al. [19] is contemporary to that of Ravi and proposed similar runtime approaches to divisible workloads. The work by Bosilca et al. [17] presented DAGuE, a framework to enable the use of heterogeneous accelerated machines to executed dense linear algebra operations.

Our solution combines the coarse-grain dataflow pattern with the bag-of-tasks pattern in order to facilitate the implementation of an analysis application from a set of processing components. It supports hierarchical pipelines, in which a processing component can itself be a pipeline of operations, and implements optimizations for efficient use of CPUs and GPUs in coordination on a computing node. The runtime optimizations include data locality conscious and performance variation aware task assignment, data prefetching, asynchronous data copy, and architecture aware placement of control processes in a computation node. Fine-grain operations that constitute an analysis pipeline typically involve different data access and processing patterns. Consequently, variability in the amount of GPU acceleration of operations is likely to exist. This requires the use of performance aware scheduling techniques in order to optimize the use of CPUs and GPUs based on speedups attained by each operation. In addition, our middleware automatically applies data locality conscious task

assignment to ensure good performance even in the case where performance variability is not present or speedup estimates are not available. Data prefetching and asynchronous data transfers between CPUs and GPUs are also employed in order to maximize the GPU utilization and reduce data copy overheads by enabling data flow between devices in parallel to ongoing computation. We demonstrate the application of the runtime system via the implementation of a biomedical image analysis application, used in study of brain tumors. We carry out a performance evaluation of the runtime system on a state-of-the-art distributed memory cluster machine where each node has two 6-core CPUs and 3 high-end GPUs.

## II. APPLICATION SCENARIO

Biomedical research studies that make use of large datasets of digital microscopy images are a good example of scientific applications targeted in our work. An example of such studies is the work done at the In Silico Brain Tumor Research Center (ISBTRC) [26], [27]. ISBTRC conducts research on brain tumors, to find better tumor classification strategies and to understand the biology of brain tumors, using complementary datasets of high-resolution whole tissue slide images (WSIs), gene expression data, clinical data, and radiology images. As part of this research effort, our group has developed image analysis applications to extract and classify morphology and texture information from high resolution WSIs, with the objective of exploring correlations between tissue morphology features, genomic signatures, and clinical data [28], [29]. The WSI analysis applications share a common set of cascaded stages, including: 1) image preprocessing tasks such as color normalization, 2) segmentation of micro-anatomic objects such as cells and nuclei, 3) characterization of the shape and texture features of the segmented objects, and 4) machine-learning methods that integrate information from features to classify the objects. In terms of computation cost, the preprocessing and classification stages (stages 1 and 4) are inexpensive relative to the segmentation and feature computation stages (stages 2 and 3). The classification stage includes significant data reduction prior to the actual classification operation which reduces computational requirements. The segmentation and feature computation stages, on the other hand, may operate on hundreds of images with resolutions ranging from  $50K \times 50K$  to  $100K \times 100K$  pixels and  $10^5$  to  $10^7$  micro-anatomic objects (e.g., cells and nuclei) per image. Our optimization efforts to date, therefore, have been focused on these two stages.

The segmentation stage detects cells and nuclei and delineates their boundaries. It consists of several component operations, forming a coarse-grain dataflow graph (see Figure 1). The operations include morphological reconstruction to identify candidate objects, watershed segmentation to separate overlapping objects, and filtering to eliminate candidates that are unlikely to be nuclei based on object characteristics. The feature computation stage derives quantitative attributes in the form of a feature vector for the entire image or for individual segmented objects. The feature types include pixel statistics, gradient statistics, Haralick features [30], edge, and morphom-

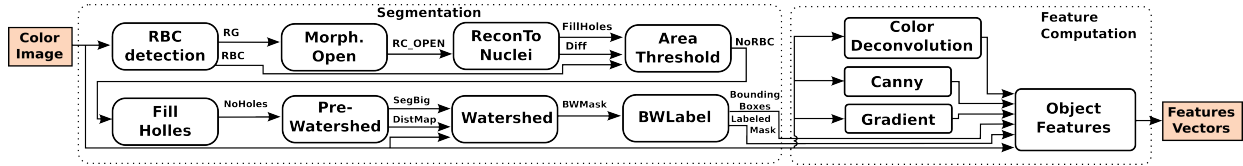


Fig. 1. Pipeline for segmenting nuclei in a whole slide tissue image and computing their features. The input to the pipeline is an image or image tile. The output is a set of features for each segmented nucleus.

entry. Most of the features can be computed concurrently in a multi-threaded or parallel environment.

This application scenario encapsulates several processing patterns. First, each image can be partitioned into rectangular tiles, and the pre-processing, segmentation, and feature computation stages can be executed on each tile independently. This leads to a bag-of-tasks style processing pattern. Similarly, feature computations for individual objects can also be executed in this pattern. Second, the processing of a single tile is expressed as a hierarchical coarse-grain dataflow pattern. The pre-processing, segmentation, and feature computation stages are the first level of the dataflow structure. The segmentation stage itself consists of a pipeline of operations. Third, the classification stage can be expressed as a MapReduce computation, in which feature vectors for individual objects are aggregated to form average feature vectors per image and per patient. These average feature vectors are then used in machine-learning algorithms, such as k-means [31], to classify patients and images into groups.

In this paper we target the segmentation and feature computation stages. As part of our overall effort to scale the application, we also have been developing CPU and GPU versions of the components in the segmentation stage as well as those in the feature computation stage. We have used CPU and GPU implementations from the OpenCV library [32] or from other research groups such as in the case of the watershed segmentation [33]. For those operations for which we could not find existing implementations, we have developed our own implementations. Table I in Section V summarizes the source of the CPU/GPU implementations. Having CPU and GPU versions of the data processing components allows the runtime system to utilize CPU cores and GPUs on a computation node concurrently in a coordinated way, as shall be described in the next sections.

### III. MIDDLEWARE RUNTIME FRAMEWORK

#### A. Application Representation

The application representation model draws from DataCutter [7], which is a filter-stream middleware framework. An analysis application is represented as a pipeline of operations. The application operations are connected through logical streams; an operation reads data from one or more streams, processes the data, and writes the results to one or more streams. We have adapted the DataCutter application model in our framework in the following ways.

The new framework supports hierarchical pipelines in that an operation can itself be made up of a pipeline of lower-level operations. We will describe the framework in the context of two pipeline levels for the sake of presentation, although

the framework allows for multiple levels of hierarchies. The first level is the *coarse-grain operations* level, which represents the main stages of an analysis application. The *fine-grain operations* level is the second level and represents lower-level operations, from which a main stage is created. Figure 2 illustrates the hierarchical pipeline representation of an analysis application. The top of the figure shows the coarse-grain operations, while the fine-grain level is displayed in the bottom portion of the figure. In the example image analysis application, for instance, the segmentation and feature computation stages constitute the first level, whereas individual operations in those stages are represented in the second level.

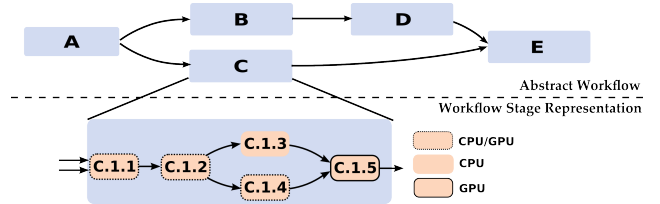


Fig. 2. Hierarchical pipeline model.

The framework distinguishes between two representations of a pipeline. The *Abstract Workflow* representation describes the logical stages of the analysis application and the connections, or dependencies, between the stages. The *Concrete Workflow* representation, on the other hand, is a binding of the logical stages and operations to actual operations and input data. The concrete workflow is in essence an instantiation of the abstract workflow representation. A *stage instance* is represented by a tuple,  $(input\ data\ chunk, processing\ stage)$ ; similarly, an *operation instance* is represented by a tuple,  $(input\ data\ chunk, operation)$ . When a stage or operation is instantiated, the dependencies that are expressed in the abstract workflow are exported to the runtime environment for correct execution. Two examples of *Concrete Workflow* instantiations of the *Abstract Workflow* in Figure 2 are presented in Figure 3.

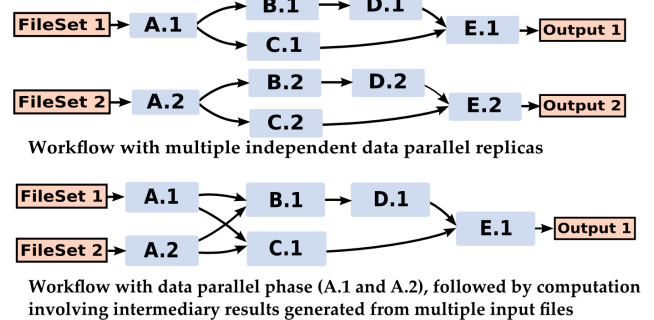


Fig. 3. Examples of *Concrete Workflow* instantiations.

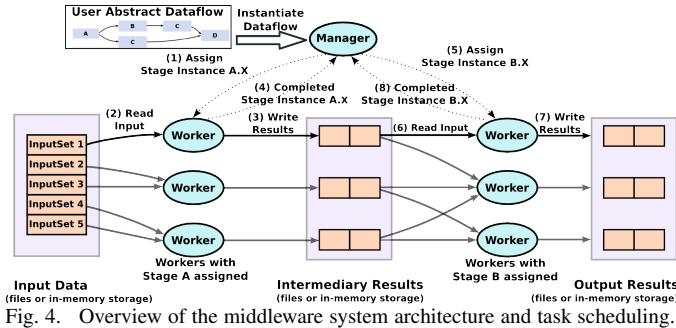
The framework makes use of the concept of function

variants to leverage CPUs and GPUs in the computing system. A function variant is a group of functions with same name, arguments, and result types [34], [15]. When a logical stage or operation is bound to a concrete operation, the concrete operation can be a single function or a function variant. In our implementation a function variant for a data processing operation is the CPU and GPU implementations of the operation. Binding to a function variant enables the runtime system to choose the appropriate function or functions during execution, allowing multiple computing devices to be used concurrently and in a coordinated manner. Note that the concept of function variants is more comprehensive, and several variants of an operation for the same computing device can coexist.

### B. Runtime System Implementation

The hierarchical representation lends itself to a separation of concerns and enables the use of different scheduling approaches at each level. For instance, it allows for the possibility of exporting second level operations (*fine-grain operations*) to a local scheduler on a hybrid node, as opposed to describing each pipeline stage as a single monolithic task, while employing a different mapping and scheduling approach for the first level. In this way, the scheduler can control tasks in a smaller granularity and can account for performance variations across the finer grain tasks within a node, while reducing the scheduling overhead for utilization of computation nodes across the machine.

In our current implementation, the runtime system uses a Manager-Worker model, as shown in Figure 4, in order to combine the bag-of-tasks style execution with the coarse-grain dataflow execution pattern.

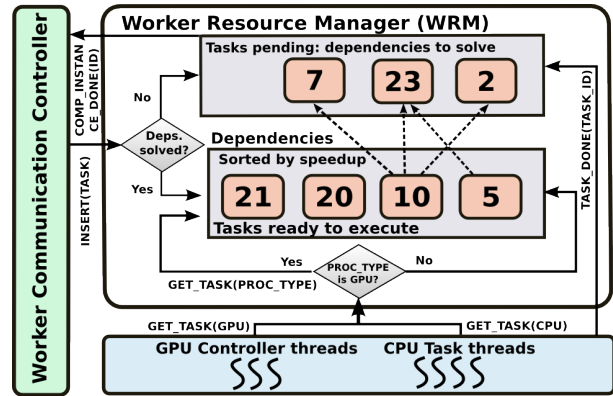


The Manager has an overall view of the runtime environment and is responsible for instantiating an abstract workflow and tracking dependencies between the workflow stages to ensure correct execution. An abstract workflow can be instantiated in several ways to take advantage of distributed computing power on a cluster system. If a dataset is divided into data chunks (e.g., image tiles in an image dataset) and each tile can be processed independently, the entire pipeline can be replicated across the system. Each replica is assigned to one or a group of nodes and processes a subset of data chunks. This type of instantiation is shown at the top of Figure 3. An alternative approach is to instantiate and execute different numbers of copies of individual stages or operations. This approach could be beneficial when some of the stages are

substantially more expensive than the other stages. This type of instantiation is illustrated at the bottom of the figure. In this example, the output of the computation performed by the instances of the stage A (stage instances A.1 and A.2) in different input data partitions is used as input to stage instances B.1 and C.1. In our implementation, the Manager can support both types of instantiations.

The granularity of tasks assigned to Worker nodes is equal to stage instances, i.e., (input data chunk, processing stage) tuples. The scheduling of tasks to Workers is carried out using a demand-driven approach. Stage instances are assigned to Workers for execution in the same order the instances are created, and the Workers continuously request work to execute as they finalize the execution of the previous instance (see Figure 4). In practice, a single worker may execute multiple application stages concurrently, and the sets of Workers shown in Figure 4 are not necessarily disjoint. Any necessary inter-process communication is done using MPI [35].

Since a Worker may use a number of CPU cores and GPUs, it may ask for multiple stage instances from the Manager in order to keep all computing devices busy. The maximum number of stage instances assigned to a Worker at a time is a configurable value (*Window size*). The Worker may request multiple stage instances in one request or in multiple requests; in the latter case, the assignment of a stage instance and the retrieval of necessary input data chunks can be overlapped with the processing of an already assigned stage instance.



Each Worker is capable of utilizing all computing devices available within a single node. The Worker Communication Controller (WCC) module runs on one of the CPU cores and is responsible for performing any necessary communication with the Manager. All computing devices used by a Worker are controlled by a local Worker Resource Manager (WRM). When a Worker receives a stage instance from the Manager and if the stage instance is composed of a pipeline of finer-grain operations, the Worker instantiates each of the operations in the form of (input data, operation) tuples, and dispatches the tuples to the local WRM for execution – if

Workers are implemented as multithread processes (see Figure 5). Each Worker is capable of utilizing all computing devices available within a single node. The Worker Communication Controller (WCC) module runs on one of the CPU cores and is responsible for performing any necessary communication with the Manager. All computing devices used by a Worker are controlled by a local Worker Resource Manager (WRM). When a Worker receives a stage instance from the Manager and if the stage instance is composed of a pipeline of finer-grain operations, the Worker instantiates each of the operations in the form of (input data, operation) tuples, and dispatches the tuples to the local WRM for execution – if

the stage instance is a single operation, it is dispatched to the WRM as if it were a single step pipeline. The WRM maps the (input data, operation) tuples to the local computing devices as the dependencies between the operations are resolved. In this model of a Worker, one computing thread is assigned to manage each available CPU computing core or a GPU. The threads notify the WRM whenever they become idle. The WRM then selects one of the tuples ready for execution for that particular thread. The function variant is used at this point to select the appropriate operation implementation based on the type of the computing device.

When all the operations in the pipeline related to a given stage instance are executed, a callback function is invoked to notify the WCC. The WCC then notifies the Manager about the end of that stage instance and requests more stage instances.

#### IV. RUNTIME OPTIMIZATIONS

The baseline approach used by the WRM to decide which tuple should be executed next is based on a First-Come-First-Served (FCFS) approach. In this approach, the WRM maintains a FIFO queue of tuples. It selects the next tuple to be executed from the head of the queue and assigns it to the next available computing device. The Worker process adds to this queue new tuples as it receives more work from the Manager. In this section, we present several runtime optimizations that improve on this baseline strategy.

##### A. Architecture Aware Threads placement

Machines with multiple multi-core CPUs and multiple GPUs may have heterogeneous configurations of data paths between CPUs and GPUs to reduce bottlenecks in data transfers between these devices. An example is the Keeneland system [2] used in our experimental evaluation. Each node in Keeneland is built using three GPUs and two multi-core CPUs, which are connected to each other through a NUMA (Non Uniform Memory Architecture) configuration. In this configuration, there are multiple I/O hubs, and the number of links traversed to access a GPU varies based on the CPU used by the calling process (see Figure 6).

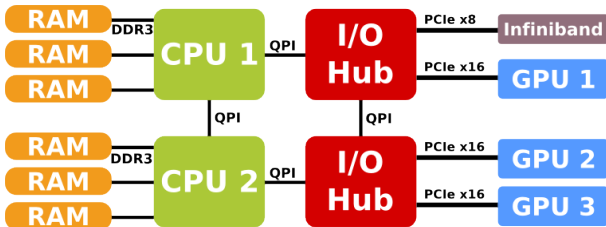


Fig. 6. Architecture of a Keeneland node.

To use these multiple I/O hubs efficiently, it is important that CPU threads responsible for managing GPUs be mapped to appropriate CPU cores. In our implementation, the placement is done such that the minimum number of links is traversed to access a given GPU. In other words, on a Keeneland node, CPU 1 manages GPU 1, while the thread controllers of GPU 2 and GPU 3 are mapped to CPU 2. This thread assignment is referred to as *Closest* in performance evaluation in the experimental results section.

##### B. Performance Aware Task Scheduling (PATS)

Stage instances assigned to a Worker may create many finer-grain operation instances. The operation instances need to be mapped to available CPU cores and GPUs efficiently in order to fully utilize the computing capacity of a node. Several recent efforts on task scheduling in heterogeneous environments have targeted machines equipped with CPUs and GPUs [15], [14], [16]. These works address the problem of partitioning and mapping tasks between CPUs and GPUs for applications in which operations (or tasks) achieve consistent and data-independent speedups when executed on a GPU vs on a CPU. The previous efforts differ mainly in whether they use off-line, on-line, or automated scheduling approaches. However, when there are multiple types of operations in an application, the operations may have different processing and data access patterns and attain different amounts of speedup on a GPU. Even for the same operation, input data characteristics may result in performance variability; the same operation may achieve different speedup values with different data chunks.

In order to use performance variability to our advantage, we have developed a strategy, referred here to as *PATS* (formerly *PRIORITY* scheduling) [36]. This strategy assigns tasks to CPU cores or GPUs based on an estimate of the relative performance gain of each task on a GPU compared to its performance on a CPU core and on the computational loads of the CPUs and GPUs. We briefly describe the strategy here. We refer the reader to our earlier publication [36] for more details and a discussion and evaluation of performance aware task scheduling in the context of independent tasks. In this work, we have extended the *PATS* scheduler to take into account dependencies between operations in an analysis workflow.

The *PATS* scheduler uses a queue of operation instances, i.e., (*data element, operation*) tuples, sorted based on the relative speedup expected for each tuple. As more tuples are created for execution with each Worker and pending operation dependencies are resolved, more operations are queued for execution. Each new operation is inserted in the queue such that the queue remains sorted (see Figure 5). During execution, when a CPU core or GPU becomes idle, one of the tuples from the queue is assigned to the idle device. If the idle device is a CPU core, the tuple with the minimum estimated speedup value is assigned to the CPU core. If the idle device is a GPU, the tuple with the maximum estimated speedup is assigned to the GPU. The *PATS* scheduler relies on maintaining the correct relative order of speedup estimates rather than the accuracy of individual speedup estimates. Even if the speedup estimates of two tasks are not accurate with respect to their respective real speedup values, the scheduler will correctly assign the tasks to the computing devices on the node, as long as the order of the speedup values is correct.

##### C. Data Locality Conscious Task Assignment (DL)

GPU equipped machines are built with an extra level in the memory hierarchy, because discrete GPUs typically have their own memory subsystem. Input data for and output data from an operation may have to be transferred back-and-

forth between CPU and GPU as operations in a pipeline are scheduled to CPUs and GPUs. The benefits of using a GPU for a certain computation may be strongly impacted by the cost of data transfers between a GPU and a CPU before the GPU kernel can be started for computation. The data transfer overheads are determined by the location where the input data resides, and where the output data will be stored [37].

In our execution model, input and output data are well defined as they refer to the input and output streams of each stage and operation, which are used by the downstream stages and operations in the analysis pipeline. Leveraging this structure, we extend the scheduler, which in basic operation mode uploads and downloads the input and output data used by an operation for each assignment, with the concept of locality in order to promote data reuse and avoid penalties due to excessive data movement. After an operation assigned to a GPU has finished, the scheduler explores the operation dependency graph and searches for operations ready for execution that can reuse the data already in the GPU memory.

If the operation speedups are not known, the scheduler always chooses to reuse data instead of selecting another operation that do not reuse data, since the scheduler will not be able to choose a better task for GPU execution without the speedup estimates. For the case where speedup estimates for operations are available, the scheduler searches for tasks that reuse data in the dependency graph, but it additionally takes into consideration other operations ready for execution. Although those operations may not reuse data, it may be worthwhile to pay the data transfer penalties if they benefit more from execution on a GPU than the operations that can reuse the data. To choose which operation instance to execute in this situation, the speedup of the dependent operation with best speedup ( $S_d$ ) is compared to that of the operation with the best speedup ( $S_q$ ) in the queue that does not reuse the data. The dependent operation is chosen for execution, if  $S_d \geq S_q \times (1 - transferImpact)$ . Here  $transferImpact$  is a value between 0 and 1 and represents the fraction of the operation execution time spent in data transfer.

#### D. Data Prefetching and Asynchronous Data Copy

Data locality conscious task assignment reduces data transfers between CPUs and GPUs for successive operations in a pipeline. However, there are moments in the execution when data still have to be exchanged between these devices because of scheduling decisions. In those cases, data copy overheads can be reduced by employing pre-fetching and asynchronous data copy. The typical execution of a GPU application involves a cyclic communication pattern, in which data elements are copied to the GPU, the computation *kernel* is launched, and output data elements are copied to the CPU memory. This communication pattern tends to be much slower than acyclic patterns, in which data can be copied to the GPU in parallel to the execution of the computation *kernel* on a previously copied data [38]. In a similar way, results from previous computations may be copied to the CPU in parallel to a *kernel* execution. In order to employ both data prefetching

Pipeline operation	CPU source	GPU source
RBC detection	OpenCV and Vincent [39] Morph. Reconstruction (MR)	Implemented
Morph. Open	OpenCV (by a 19x19 disk)	OpenCV
ReconToNuclei	Vincent [39] MR	Implemented
AreaThreshold	Implemented	Implemented
FillHolles	Vincent [39] MR	Implemented
Pre-Watershed	Vincent [39] MR and OpenCV for distance transformation	Implemented
Watershed	OpenCV	Korbes [33]
BWLabel	Implemented	Implemented
Features comp.	Implemented.	Implemented.
	OpenCV(Canny)	OpenCV(Canny)

TABLE I  
SOURCES OF CPU AND GPU IMPLEMENTATIONS OF OPERATIONS IN THE SEGMENTATION AND FEATURE COMPUTATION STAGES.

and asynchronous data copy, we modified the runtime system to perform the computation and communication of pipelined operations in parallel. The execution of each operation using a GPU in this execution mode involves three phases: *uploading*, *processing*, and *downloading*. Each GPU manager thread and WRM pipeline multiple operations through these three phases. Any input data needed for another operation waiting to execute and the results from a completed operation are copied from and to the CPU in parallel to the ongoing computation in the GPU.

## V. EXPERIMENTAL EVALUATION

### A. Experimental Setup

We have evaluated the proposed runtime system and optimizations using a distributed memory hybrid cluster, called Keeneland [2]. Keeneland is a National Science Foundation Track2D Experimental System and has 120 nodes in the current configuration. Each computation node is equipped with a dual socket Intel X5660 2.8 Ghz Westmere processor, 3 NVIDIA Tesla M2090 (Fermi) GPUs, and 24GB of DDR3 RAM (See Figure 6). The nodes are connected to each other through a QDR Infiniband switch.

We used the example application described in Section II for performance evaluation. The segmentation and feature computation stages were implemented as a coarse-grain workflow with two levels. The stages formed the first level, while the pipeline of operations in each stage formed the second level. As is described in Section II, each operation has a CPU version and a GPU version. Several of the compute intensive operations along with the sources of the CPU/GPU implementations are listed in Table I. We used existing implementations from OpenCV or from other research groups, or implemented our own if no efficient implementations were available. The Morphological Open operation, for example, is available as part of OpenCV [32] that uses NVidia Performance Primitives (NPP) [40]. The Watershed operation, on the other hand, has only a CPU implementation in the OpenCV library. We used the GPU implementation by Korbes et. al. [33] for this operation. We should note that the internal algorithms used by OpenCV and Korbes' implementations are not the same; hence, the results from the CPU and GPU implementations are slightly different. Several of the operations in the segmentation stage are irregular computations. The Morphological Reconstruction (MR) algorithm, which is used in these operations,

has a fast CPU implementation using wave-propagation based computation approach [39]. We have implemented a hierarchical queue-based wave-propagation framework to accelerate the MR algorithm, and the operations that use MR, on a GPU. The details of the framework is available as a technical report [41]. The queue-based implementation resulted in significant performance improvements over previously published versions of the MR algorithm [42]. Operations in the feature computation stage implement a number of pixel/neighborhood based transformations that are applied to the input image (Color deconvolution, Canny, and Gradient). Object features are extracted from the results of the computations, based on object boundaries determined in the segmentation stage. Object feature computations are generally more regular and compute intensive than the operations in the segmentation stage. This characteristics of the feature computation operations lead to better GPU acceleration.

Image datasets used in the evaluation were obtained from studies in the In Silico Brain Tumor Research Center [27]. Each image was partitioned into tiles of  $4K \times 4K$  pixels. The codes were compiled using “gcc 4.1.2”, “-O3” optimization flag, OpenCV 2.3.1, and NVIDIA CUDA SDK 4.0. The experiments were repeated 3 times. The standard deviation in performance results was not observed to be higher than 2%. The input data were stored in the Lustre filesystem, which is shared among multiple users.

### B. Performance of Application Operations on GPU

This section presents the performance gains on GPU of the pipeline operations. Figure 7 shows the performance gains achieved by each of the fine-grain operations in the second level of the pipeline, as compared to the single core CPU counterpart. The speedup values in the figure represent the performance gains (1) when only the computation phase is considered (computation-only) and (2) when the cost of data transfer between CPU and GPU is included (computation+data transfer). The figure also shows the percentage of the overall computation time spent in an operation on one CPU core.

The results show that there are significant variations in performance gains among operations, as expected. The most time consuming stages are the ones with the best speedup values – this is in part because of the fact that we have focused on optimizing the GPU implementations of those operations to reduce overall execution time. The feature computation stage stands out as having better GPU acceleration than the segmentation stage. This is a consequence of the former stage’s more regular and compute intensive nature.

Our evaluation indicates that the task scheduling approach should take into consideration these performance variations to maximize performance on hybrid CPU-GPU platforms. We evaluate the performance impact on pipelined execution of using PATS for scheduling operations in Section V-D.

### C. Architecture Aware Placement of Control Threads

We employed two strategies for placement of CPU threads responsible for managing the GPUs on a cluster node. The strategies used are: (i) OS: refers to the placement chosen

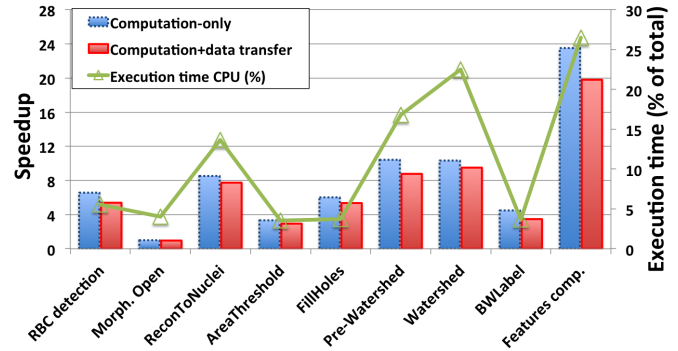


Fig. 7. Evaluation of the GPU-based implementations of application components (operations).

automatically by the Operation System; and, (ii) Closest: binds a CPU thread managing a GPU closest to that GPU regarding to the number of connections that need to be traversed to access the GPU (Section IV-A). Three randomly selected images were used as input in the experiments. Each image contains  $56K \times 56K$  pixels and is partitioned into 196  $4K \times 4K$ -pixel image tiles. Tiles with background only pixels were discarded beforehand, resulting in about 100 tiles per image. The image tiles are stored in files. The speedup results presented in this section include the time taken to read the input data from the Lustre filesystem.

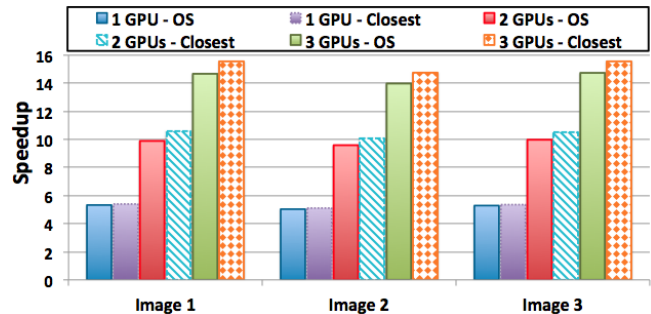


Fig. 8. Speedups on end-to-end execution using multiple GPUs and different control thread placement strategies. The results include disk I/O overheads to read image tiles.

The performance impact of the two strategies when the number of GPUs is varied as shown in Figure 8. The end-to-end acceleration of the pipeline using a single GPU is about  $5.3 \times$  for both placement strategies, as compared to the single core CPU version. Although a number of operations in the pipeline achieve better speedups, the ones with lower speedups will limit the overall gains. For instance, Morphological Open accounts for about 4% of the CPU execution time, but it represents about 23% of the computation time for the GPU accelerated version. In addition, the results also include time spent in reading the input data which is another performance limiting factor. If only the computation phase were considered, the GPU speedups would be about  $1.22 \times$  higher than what is reported (i.e., about  $6.5 \times$  better performance compared to one CPU core).

Figure 8 also shows the performance of the pipeline in multi-GPU configurations. The appropriate assignment of

threads managing the GPUs — *Closest* — achieved similar or superior performance than the *OS* for all experiments. The *Closest* placement gains are higher as the number of GPUs increases: about 3%, 6%, and 8% better performance for the 1-, 2-, and 3-GPU configurations, respectively, in comparison to *OS*. This performance is consistent across the experiments done using each of the three images. The *Closest* placement is used in the rest of the experiments involving GPUs.

#### D. Pipeline Execution using CPUs and GPUs in Coordination

This section presents the experimental results when multiple CPU cores and GPUs are used together to execute the analysis workflow. In these experiments, two versions of the application workflow are used: (i) *pipelined* refers to the version described in Section II, where the operations performed by the application are organized as a hierarchical pipeline; (ii) *non-pipelined* that bundles the entire computation of an input tile as a single monolithic task, which is executed either by CPU or GPU. The comparison between these versions is important to understand the performance impact of pipelining application operations.

Two scheduling strategies were employed for mapping tasks to CPUs or GPUs: (i) FCFS which does not take performance variation into consideration; and, (ii) PATS that uses the expected speedups achieved by an operation in the scheduling decision. When PATS is used, the speedup estimates for each of the operations are those presented in Figure 7.

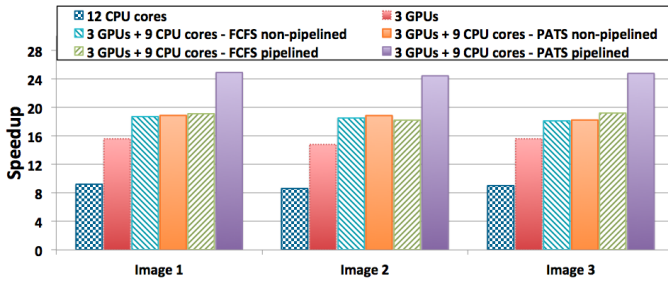


Fig. 9. Application scalability when multiple CPUs and GPUs are used via the PATS and FCFS scheduling strategies.

The results for the various configurations are presented in Figure 9, using the three images from the experiments in the previous section. In all cases, the CPU speedup using 12 cores is about 9. The sub-linear speedups are a result of the application’s high memory bandwidth requirements. The 3-GPU execution achieved near linear scalability for all images. The coordinated use of CPUs and GPUs improved performance over the 3-GPU executions. We should note that only upto 9 CPU cores are used in the multi-device experiments, because 3 cores are dedicated to GPU control threads. In the non-pipelined version of the application, potential performance gains by using CPUs and GPUs together are limited by load imbalance. If a tile is assigned to a CPU core near the end of the execution, the GPUs will sit idle waiting until the CPU core finishes, which reduces the benefits of cooperated use of computing devices. The performance of PATS for the non-pipelined version is similar to FCFS. In this case, the PATS scheduling is not able to make better decisions than FCFS,

because the non-pipelined version bundles all the internal operations of an application stage as a single task, hence the performance variations of the operations are not exposed to the runtime system.

The CPU-GPU execution of the pipelined version of the application with FCFS (3 GPUs + 9 CPU cores - FCFS pipelined) also improved the 3-GPU execution, reaching similar performance to that of the non-pipelined execution. This version of the application requires that the data are copied to and from a GPU before and after an operation in the pipeline is assigned to the GPU. This introduces a performance penalty due to the data transfer overheads, which are about 13% of the computation time as show in Figure 7, and limits the performance improvements of the pipelined version. The advantage of using the pipelined version in this situation is that load imbalance among CPUs and GPUs is reduced. The assignment of computation to CPUs or GPUs occurs at a finer-grain; that is, application operations in the second level of the pipeline make up the tasks scheduled to CPUs and GPUs, instead of the entire computation of a tile as in the non-pipelined version.

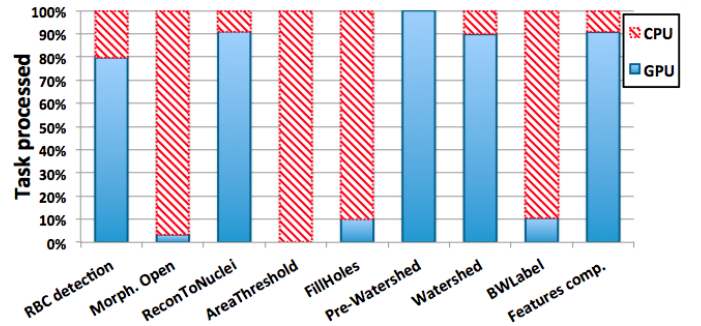


Fig. 10. Execution profile (% of tasks processed by CPU or GPU) using PATS per pipeline stage.

Figure 9 also presents the performance of the PATS scheduling for the pipelined version of the application. As is seen from the figure, processing of tiles using PATS is about  $1.33\times$  faster than using FCFS with the non-pipelined or pipelined version of the application. The performance gains result from the ability of PATS to better assign the application internal operations to the most suited computing devices. For instance, Figure 10 presents the percent of tasks that PATS assigned to the CPUs or GPUs for each pipeline stage. As is shown, the execution of components with lower speedups are mostly performed using the CPUs, while the GPUs are kept occupied with operations that achieve higher speedups. For reference, using FCFS with the pipelined version, the operations are more or less evenly distributed across CPUs and GPUs regardless of performance variations between the operations.

#### E. Data Locality Conscious Scheduling and Data Prefetching

In this section, we evaluate the performance impact of the data locality conscious task assignment (DL) and data prefetching and asynchronous data download (Prefetching) optimizations. Figure 11 presents the performance improvements with these optimizations for both PATS and FCFS policies. As



is shown, the pipelined version with FCFS and DL is able to improve the performance of the non-pipelined version by about  $1.1\times$  for all input images. When Prefetching is used in addition to FCFS and DL (“3GPUs + 9 CPU core - pipelined FCFS + DL + Prefetching”), there are no significant performance improvements. The main reason is that DL already avoids any unnecessary CPU-GPU data transfers; therefore, Prefetching will only be effective in reducing the cost of uploading the input tile to the GPU and downloading the final results from the GPU. These costs are small and limit the performance gains resulting from Prefetching.

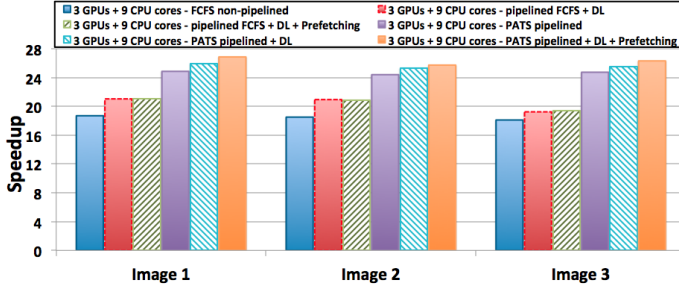


Fig. 11. Performance impact of data locality conscious mapping and asynchronous data copy optimizations.

Figure 11 also shows the performance results for PATS when DL and Prefetching are employed. The use of DL improves the performance of PATS as well, but the gains achieved ( $1.04\times$ ) with DL are smaller than those in FCFS. In this case, the estimated speedups for the operations are available, thus PATS will check whether it is worthwhile to download the operation results to map another operation to the GPU. The number of upload/downloads avoided by using DL is also smaller than when FCFS is used, which explains the performance gain difference. Prefetching with DL results in an additional  $1.03\times$  performance improvement. This optimization was more effective in this case because the volume of data transferred between the CPU and the GPU is much higher than when FCFS with DL is employed.

### F. Impact of Worker Request Window Size

This section analyzes the effect of the demand-driven window size between Manager and Workers (i.e., the number of pipeline stage instances concurrently assigned to a Worker) on the CPU-GPU scheduling strategies utilized by the Worker. During this evaluation, we used 3 GPUs and 9 CPU cores (with 3 CPU cores allocated to the GPU manager threads) with FCFS and PATS. The window-size is varied from 12 until no significant performance changes are observed.

	Demand-Driven Window Size							
	12	13	14	15	16	17	18	19
FCFS	75.1	73.4	74.9	73.7	75.3	74.9	73.2	73.5
PATS	75.1	61	56.9	53.1	54.1	51.5	51.2	50.7

TABLE II

EXECUTION TIME (SECS.) FOR DIFFERENT REQUEST WINDOW SIZE AND SCHEDULING POLICIES USING 3 GPUS AND 9 CPU CORES.

Table II presents the execution times. FCFS scheduling is impacted little by variation in the window size. The PATS

scheduler performance, on the other hand, is limited for small window sizes. In the scenario where the window size is 12, FCFS and PATS tend to make the same scheduling decisions, because only a single operation will be available when a processor requests work. This makes the decision trivial and equal for both strategies. When the window size is increased, however, the scheduling decision space becomes larger, providing PATS with opportunities to make better task assignments. As is shown in the table, with a window size of 15, PATS already achieves near its best performance. This is another good property of PATS, since very large window sizes can create load imbalance among Workers.

The profile of the execution (% of tasks processed by GPU) as the window size is varied is displayed in Figure 12. As the window size increases, PATS quickly changes the assignment of tasks, and operations with higher speedups are more likely to be executed by GPUs. FCFS profile is not presented in the same figure, but its profile is similar to PATS with a window size of 12 for all configurations.

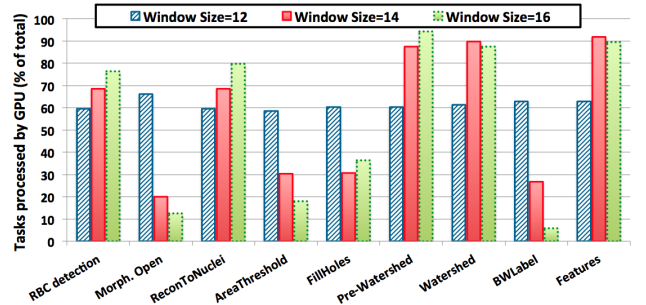


Fig. 12. Execution scheduling profile for different window sizes and the PATS strategy.

### G. Effects of Inaccurate Speedup Estimation

In this section, we empirically evaluate the sensitivity of PATS scheduler to errors in the GPU-vs-CPU speedup estimation of operations. For the sake of this analysis, we intentionally inserted errors in the estimated speedup values of the application operations in a controlled manner. In order to effectively confound the method, operations with lower speedups that are mostly scheduled to the CPUs (Morph. Open, AreaThreshold, FillHoles, and BWLabel; see Figure 10) had their estimated speedup values increased, while the others have the values decreased. The changes are calculated as a percentage of an operation’s original estimated speedup, and the variation range was from 0% to 100%.

The execution times for different error rates are presented in Figure 13. The results show that PATS is capable of performing well even with high errors and error rates in speedup estimations. For instance, when 60% estimation error is used, the performance of the pipeline is only 10% worse than the initial case (0% speedup estimation error). At 70% and 80% errors, PATS performance is more impacted, as a result of a miss-ordering of the pipeline operations before mostly processed by CPU (AreaThreshold, FillHoles, and BWLabel) with ReconToNuclei and Watershed. Consequently,

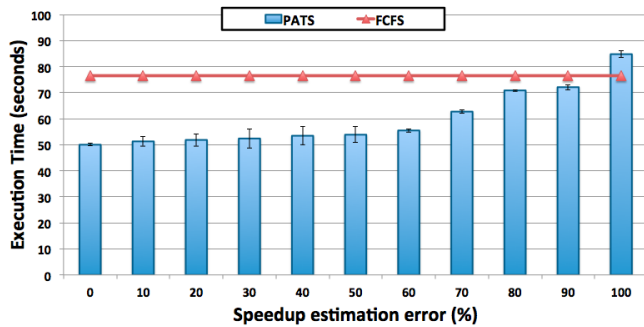


Fig. 13. Performance of PATS when errors in speedup estimation for the pipeline operations are introduced.

those stages with lower speedups will be scheduled for execution on a GPU. Nevertheless, PATS still performs better than FCFS, because the operations in the feature computation stage are not miss-ordered. To emulate 100% estimation error, we set to 0 the speedups of all substages that in practice have higher speedups, and double the estimated speedups of the other stages that in reality have lower speedup values. This forces PATS to preferably assign operations with low speedups to GPU and the ones with high speedup to CPU. Even with this level of error, the execution times are only about 10% worse than those using FCFS.

#### H. Multi-node Scalability

This section presents the performance evaluation of the runtime system when multiple computation nodes are used. The evaluation was carried out using 340 glioblastoma brain tumor WSIs, which were partitioned into a total of 36,848  $4K \times 4K$  tiles. Figure 14 shows the execution times for all configurations when the number of computing nodes is varied from 8 to 100. As in the other experiments, the input tiles were stored in the Lustre filesystem. As is shown in the figure, PATS with the other optimizations achieved the best performance with a speedup of  $1.3 \times$  over FCFS. The efficiency of the runtime system on 100 nodes is about 77%. The main limiting factor and bottleneck is the I/O overhead of reading image tiles. As the number of nodes increases, I/O operations become more expensive, because more clients access the file system in parallel. If only the computation times were measured, the efficiency would increase to about 93%. Even with the I/O overheads, the runtime system was able to process the entire set of 36,848 tiles in less than four minutes when 100 nodes were used. This represents a huge improvement in computing capabilities; the same computation would take days or weeks on a workstation using the original MATLAB version.

## VI. CONCLUSIONS

Hybrid CPU-GPU cluster systems offer significant computing and memory capacity to address the computational needs of large scale scientific analyses. We have developed a middleware system to tap this capacity and enable high-throughput data processing by leveraging common data access and processing patterns in scientific analysis applications. Findings from the experimental evaluation of this system on a state-of-the-art hybrid cluster system can be summarized

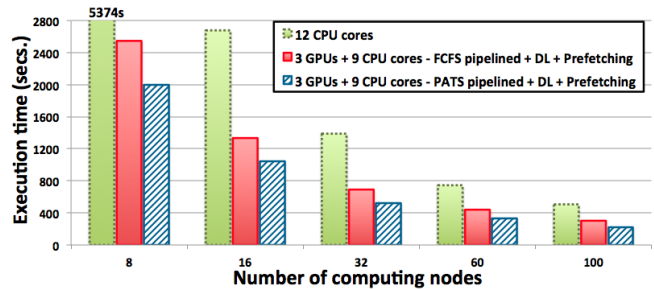


Fig. 14. Multi-node scalability: strong scaling evaluation.

as follows: Significant performance improvements can be achieved when an analysis application can be assembled as pipelines of fine-grain operations compared to bundling all internal operations in one or two monolithic methods. The former allows for exporting application processing patterns more accurately to the runtime environment and empowers the middleware system to make better scheduling decisions. Performance aware task scheduling coupled with function variants enable efficient coordinated use of CPU cores and GPUs in pipelined operations. Performance gains can further be increased on hybrid systems through such additional runtime optimizations as locality conscious task mapping, data prefetching, and asynchronous data copy. Employing a combination of these optimizations, our runtime system implementation has achieved a processing rate of about 150 tiles per second when 100 nodes are used. These levels of processing speed make it feasible to process very large datasets and would enable a scientist to explore different scientific questions rapidly and/or carry out algorithm sensitivity studies.

The work presented in this paper has focused on the segmentation and feature computation stages of the example analysis application. We plan to extend support to the classification stage. This stage implements a MapReduce style processing pattern. Moreover, although the classification stage in the current application implementation is relatively inexpensive, since it operates on aggregated image and patient level data, there are plans to extend it to support clustering-based classifications using object level data – the number of segmented nuclei in a large data set can reach hundreds of millions, even billions. We are currently in the process of developing fast CPU and GPU implementations for clustering large volumes of point data. We plan to integrate these function variants along with support for MapReduce type of processing in order to provide full support for analysis applications that are similar to the example analysis application.

**Acknowledgments.** This work was supported in part by HHSN261200800001E from the National Cancer Institute, R24HL085343 from the National Heart Lung and Blood Institute, by R01LM011119-01 and R01LM009239 from the National Library of Medicine, RC4MD005964 from National Institutes of Health, and PHS UL1RR025008 from the Clinical and Translational Science Awards program. This research used resources of the Keeneland Computing Facility at the Georgia Institute of Technology, which is supported by the National Science Foundation under Contract OCI-0910735.

## REFERENCES

- [1] NVIDIA, "GPU Accelerated Applications," 2012. [Online]. Available: <http://www.nvidia.com/object/gpu-accelerated-applications.html>
- [2] J. S. Vetter, R. Glassbrook, J. Dongarra, K. Schwan, B. Loftis, S. McNally, J. Meredith, J. Rogers, P. Roth, K. Spafford, and S. Yalamanchili, "Keeneland: Bringing heterogeneous gpu computing to the computational science community," *Computing in Science and Engineering*, vol. 13, 2011.
- [3] NVIDIA, "NVIDIA CUDA SDK," 2011. [Online]. Available: <http://nvidia.com/cuda>
- [4] Khronos OpenCL Working Group, *The OpenCL Specification, version 1.0.29*, 8 December 2008. [Online]. Available: <http://khronos.org/registry/cl/specs/opencl-1.0.29.pdf>
- [5] N. Carriero and D. Gelernter, *How to write parallel programs: a first course*. Cambridge, MA, USA: MIT Press, 1990.
- [6] J. Dean and S. Ghemawat, "MapReduce: Simplified data processing on large clusters." in *Proceedings of the Sixth Symposium on Operating System Design and Implementation (OSDI'04)*, December 2004, pp. 137–150.
- [7] M. D. Beynon, T. Kurc, U. Catalyurek, C. Chang, A. Sussman, and J. Saltz, "Distributed processing of very large datasets with DataCutter," *Parallel Comput.*, vol. 27, no. 11, pp. 1457–1478, 2001.
- [8] G. Eisenhauer, F. E. Bustamante, and K. Schwan, "Event services for high performance computing," in *Proceedings of High Performance Distributed Computing (HPDC)*, 2000.
- [9] H. Abbasi, M. Wolf, G. Eisenhauer, S. Klasky, K. Schwan, and F. Zheng, "DataStager: scalable data staging services for petascale applications," in *Proceedings of the 18th ACM international symposium on High performance distributed computing*, ser. HPDC '09. New York, NY, USA: ACM, 2009, pp. 39–48. [Online]. Available: <http://doi.acm.org/10.1145/1551609.1551618>
- [10] J. Subhlok, J. M. Stichnoth, D. R. O'Hallaron, and T. R. Gross, "Programming task and data parallelism on a multicomputer," in *PPOPP*, 1993, pp. 13–22.
- [11] G. Teodoro, D. Fireman, D. Guedes, W. M. Jr., and R. Ferreira, "Achieving multi-level parallelism in filter-labeled stream programming model," in *The 37th International Conference on Parallel Processing (ICPP)*, 2008.
- [12] G. Teodoro, T. Tavares, R. Ferreira, T. Kurc, W. Meira, D. Guedes, T. Pan, and J. Saltz, "A run-time system for efficient execution of scientific workflows on distributed environments," *Int. J. Parallel Program.*, vol. 36, no. 2, pp. 250–266, Apr. 2008. [Online]. Available: <http://dx.doi.org/10.1007/s10766-007-0068-8>
- [13] T. Tavares, G. Teodoro, T. Kurc, R. Ferreira, D. Guedes, W. J. Meira, U. Catalyurek, S. Hastings, S. Oster, S. Langella, and J. Saltz, "An efficient and reliable scientific workflow system," *IEEE International Symposium on Cluster Computing and the Grid*, vol. 0, pp. 445–452, 2007.
- [14] B. He, W. Fang, Q. Luo, N. K. Govindaraju, and T. Wang, "Mars: A MapReduce Framework on Graphics Processors," in *Parallel Architectures and Compilation Techniques*, 2008.
- [15] M. D. Linderman, J. D. Collins, H. Wang, and T. H. Meng, "Merge: a programming model for heterogeneous multi-core systems," *SIGPLAN Not.*, vol. 43, no. 3, pp. 287–296, 2008.
- [16] C.-K. Luk, S. Hong, and H. Kim, "Qilin: Exploiting parallelism on heterogeneous multiprocessors with adaptive mapping," in *42nd International Symposium on Microarchitecture (MICRO)*, 2009.
- [17] G. Bosilca, A. Bouteiller, T. Herault, P. Lemarinier, N. Saengpatsa, S. Tomov, and J. Dongarra, "Performance Portability of a GPU Enabled Factorization with the DAGuE Framework," in *2011 IEEE International Conference on Cluster Computing (CLUSTER)*, sept. 2011, pp. 395 – 402.
- [18] V. Ravi, W. Ma, D. Chiu, and G. Agrawal, "Compiler and runtime support for enabling generalized reduction computations on heterogeneous parallel configurations," in *Proceedings of the 24th ACM International Conference on Supercomputing*. ACM, 2010, p. 137146.
- [19] T. D. R. Hartley, E. Saule, and Ü. V. Çatalyürek, "Automatic dataflow application tuning for heterogeneous systems," in *HiPC*. IEEE, 2010, pp. 1–10.
- [20] X. Huo, V. Ravi, and G. Agrawal, "Porting irregular reductions on heterogeneous cpu-gpu configurations," in *18th International Conference on High Performance Computing (HiPC)*, dec. 2011, pp. 1–10.
- [21] G. Teodoro, T. D. R. Hartley, U. Catalyurek, and R. Ferreira, "Run-time optimizations for replicated dataflows on heterogeneous environments," in *Proc. of the 19th ACM International Symposium on High Performance Distributed Computing (HPDC)*, 2010.
- [22] J. C. Phillips, J. E. Stone, and K. Schulten, "Adapting a message-driven parallel application to gpu-accelerated clusters," in *Proceedings of the 2008 ACM/IEEE conference on Supercomputing*, ser. SC '08. Piscataway, NJ, USA: IEEE Press, 2008, pp. 8:1–8:9. [Online]. Available: <http://dl.acm.org/citation.cfm?id=1413370.1413379>
- [23] P. Jetley, L. Wesolowski, F. Gioachin, L. V. Kalé, and T. R. Quinn, "Scaling hierarchical n-body simulations on gpu clusters," in *Proceedings of the 2010 ACM/IEEE International Conference for High Performance Computing, Networking, Storage and Analysis*, ser. SC '10. Washington, DC, USA: IEEE Computer Society, 2010, pp. 1–11. [Online]. Available: <http://dx.doi.org/10.1109/SC.2010.49>
- [24] G. Teodoro, R. Sachetto, O. Sertel, M. Gurcan, W. M. Jr., U. Catalyurek, and R. Ferreira, "Coordinating the use of GPU and CPU for improving performance of compute intensive applications," in *IEEE Cluster*, 2009.
- [25] G. Teodoro, T. Hartley, U. Catalyurek, and R. Ferreira, "Optimizing dataflow applications on heterogeneous environments," *Cluster Computing*, vol. 15, pp. 125–144, 2012, 10.1007/s10586-010-0151-6. [Online]. Available: <http://dx.doi.org/10.1007/s10586-010-0151-6>
- [26] L. Cooper, J. Kong, D. Gutman, F. Wang, S. Cholleti, T. Pan, P. Widener, A. Sharma, T. Mikkelsen, A. Flanders, D. Rubin, E. Van Meir, T. Kurc, C. Moreno, D. Brat, and J. Saltz, "An Integrative Approach for In Silico Glioma Research," *IEEE Transactions on Biomedical Engineering*, oct. 2010.
- [27] J. Saltz, T. Kurc, S. Cholleti, J. Kong, C. Moreno, A. Sharma, T. Pan, E. V. Meir, T. Mikkelsen, A. Flanders, D. Rubin, and D. Brat, "Multi-scale, integrative study of brain tumor: In silico brain tumor research center," in *Annual Symposium of American Medical Informatics Association 2010 Summit on Translational Bioinformatics (AMIA-TBI 2010)*, Mar 2010.
- [28] L. A. Cooper, J. Kong, D. A. Gutman, F. Wang, J. Gao, C. Appin, S. Cholleti, T. Pan, A. Sharma, L. Scarpace, T. Mikkelsen, T. Kurc, C. S. Moreno, D. J. Brat, and J. H. Saltz, "Integrated morphologic analysis for the identification and characterization of disease subtypes," *J Am Med Inform Assoc.*, no. 2, pp. 317–323, 2012.
- [29] L. A. D. Cooper, J. Kong, D. A. Gutman, F. Wang, S. R. Cholleti, T. C. Pan, P. M. Widener, A. Sharma, T. Mikkelsen, A. E. Flanders, D. L. Rubin, E. G. V. Meir, T. M. Kurc, C. S. Moreno, D. J. Brat, and J. H. Saltz, "An integrative approach for in silico glioma research," *IEEE Trans Biomed Eng.*, vol. 57, no. 10, pp. 2617–2621, 2010.
- [30] R. Haralick, "Statistical and structural approaches to texture," *Proceedings of the IEEE*, vol. 67, no. 5, may 1979.
- [31] J. B. Macqueen, "Some methods of classification and analysis of multivariate observations," in *Proceedings of the Fifth Berkeley Symposium on Mathematical Statistics and Probability*, 1967, pp. 281–297.
- [32] G. Bradski, "The OpenCV Library," *Dr. Dobb's Journal of Software Tools*, 2000.
- [33] A. Körbes, G. B. Vitor, R. de Alencar Lotufo, and J. V. Ferreira, "Advances on watershed processing on GPU architecture," in *Proceedings of the 10th International Conference on Mathematical Morphology*, ser. ISMM'11, 2011, pp. 260–271. [Online]. Available: <http://dl.acm.org/citation.cfm?id=2023043.2023072>
- [34] T. Millstein, "Practical predicate dispatch," *SIGPLAN Not.*, vol. 39, pp. 345–364, October 2004.
- [35] "The Message Passing Interface (MPI)." [Online]. Available: <http://www-unix.mcs.anl.gov/mpi/>
- [36] G. Teodoro, T. M. Kurc, T. Pan, L. A. Cooper, J. Kong, P. Widener, and J. H. Saltz, "Accelerating Large Scale Image Analyses on Parallel, CPU-GPU Equipped Systems," in *26th IEEE International Parallel and Distributed Processing Symposium (IPDPS)*, 2012.
- [37] C. Gregg and K. Hazelwood, "Where is the data? Why you cannot debate CPU vs. GPU performance without the answer," in *Proceedings of the IEEE International Symposium on Performance Analysis of Systems and Software*, ser. ISPASS '11. Washington, DC, USA: IEEE Computer Society, 2011, pp. 134–144. [Online]. Available: <http://dx.doi.org/10.1109/ISPASS.2011.5762730>
- [38] T. B. Jablin, P. Prabhu, J. A. Jablin, N. P. Johnson, S. R. Beard, and D. I. August, "Automatic cpu-gpu communication management and optimization," in *Proceedings of the 32nd ACM SIGPLAN conference on Programming language design and implementation*, ser. PLDI '11. New York, NY, USA: ACM, 2011, pp. 142–151. [Online]. Available: <http://doi.acm.org/10.1145/1993498.1993516>
- [39] L. Vincent, "Morphological grayscale reconstruction in image analysis: Applications and efficient algorithms," *IEEE Transactions on Image Processing*, vol. 2, pp. 176–201, 1993.

- [40] NVIDIA, *NVIDIA Performance Primitives(NPP)*, 11 February 2011. [Online]. Available: <http://developer.nvidia.com/npp>
- [41] G. Teodoro, T. Pan, T. M. Kurc, L. Cooper, J. Kong, and J. H. Saltz, "A fast parallel implementation of queue-based morphological reconstruction using gpus," Emory University, Center for Comprehensive Informatics Technical Report CCI-TR-2012-2, January 2012.
- [42] P. Karas, "Efficient Computation of Morphological Greyscale Reconstruction," in *MEMICS*, ser. OASICS, vol. 16. Schloss Dagstuhl - Leibniz-Zentrum fuer Informatik, Germany, 2010, pp. 54–61.